Composite of Low-Density Polyethylene and Aluminum Obtained from the Recycling of Postconsumer Aseptic Packaging

Cristina M. A. Lopes, Maria Isabel Felisberti

Instituto de Química, Universidade Estadual de Campinas, CP 6154, Campinas SP, Brazil CEP 13084-971

Received 15 July 2005; accepted 11 October 2005
DOI 10.1002/app.23406
Publication online in Wiley InterScience (www.interscience.wiley.com).

ABSTRACT: The recycling process of postconsumer aseptic packaging composed of paper, low-density polyethylene (LDPE), and aluminum consists of recovering paper, the major component, through centrifugation. The remaining mixture of LDPE and aluminum, a recycled composite called PEAL, offers an interesting combination of properties, especially because of the presence of a small amount of poly(ethylene-*co*-methacrylic acid (EMAA). In this work, this composite is characterized, and the properties are compared with those of pure LDPE and EMAA, the polymers that constitute the recycled material. PEAL is around 15% aluminum particles with different shapes and sizes. The composite presents higher thermooxidative stability, higher crystallinity, lower impact resistance, and higher tensile strength than the other olefin polymers. © 2006 Wiley Periodicals, Inc. J Appl Polym Sci 101: 3183–3191, 2006

Key words: composites; mechanical properties; recycling; thermal properties

INTRODUCTION

Plastic packaging, including flexible films and rigid containers, has dominated the packaging field for a long time and nowadays constitutes the major applications for plastic resins. Besides effective cost in comparison with other materials, plastics present optical and barrier properties, density, and mechanical strength suitable for guaranteeing high practicality and quality and conservation of the product for a long time, which is mandatory for food packaging. The continuing development of new technology for plastic packaging confirms that this tendency will be continued.[1]

The main resins used for packaging are low-density polyethylene (LDPE), linear low-density polyethylene (LLDPE), high-density polyethylene (HDPE), poly(vinyl chloride), polypropylene, polystyrene, and poly(ethylene terephthalate).

Nowadays, besides single plastic containers, multilayer packaging is used for packing many different goods, especially food products such as meat, vegetables, milk and its derivatives, and juices and also cleaning products and medical-hospital devices. Most multilayer packaging contains polyethylene and its copolymers.[2]

Tetra Brik aseptic packaging, produced by Tetra Pak and used for milk packing after ultrapasteurization, is composed of three materials organized in six layers: paper (75%), LDPE (20%), and aluminum (5%). Polyethylene being an inert polymer, the adhesion of the aluminum film to the plastic layer is achieved through the introduction of a layer of an ethylene/methacrylic acid copolymer [poly(ethylene-*co*-methacrylic acid (EMAA)] with rheological properties similar to those of LDPE. The structure of this random ethylene copolymer is nonionized, and the comonomers are distributed in a nonspecific sequence along the chains.[3]

Besides being used as adhesion promoters in multilayer packaging, these copolymers are used for packaging meat and sausage because they present good thermal sealing in the presence of aqueous fluids.[4] Because of the facility of interacting strongly with several chemical groups, EMAA and other ethylene copolymers have great potential for use as compatibilizers and impact modifiers in blends and engineering plastics.[5]

In the last several years, plastic packaging has becoming the major component of the plastic waste stream because of the short time of use and the long period necessary for degradation.[6] As a result, plastic recycling is perceived as an important environmental topic.

Correspondence to: M. I. Felisberti (misabel@iqm.unicamp.br).
Contract grant sponsor: Fundação de Amparo à Pesquisa do Estado de São Paulo; contract grant number: 99/036980.
Contract grant sponsor: Conselho Nacional de Desenvolvimento Cientifico e Tecnológico; contract grant number: 479749/01-9.

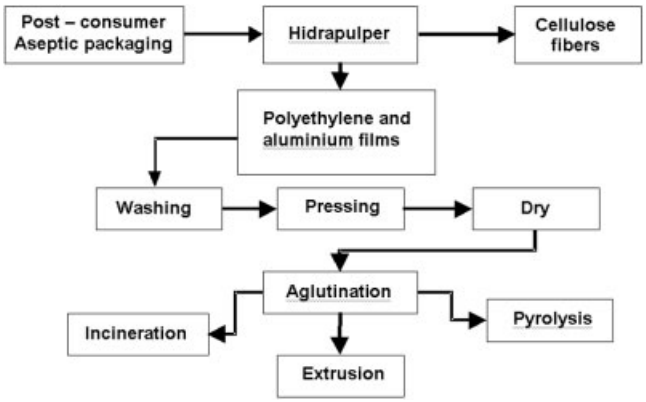

Figure 1 Recycling of the aseptic packaging.

With the increase in plastic multilayer packaging applications, the volume of these laminated products in the municipal solid waste has continuously grown. One of the recycling alternatives for packaging containing layers of different polymers is the addiction of compatibilizers during the reprocess to improve the interfacial adhesion. In the case of multilayer packaging composed of different materials such as paper, polymer, and metal, the recycling process is even more complicated.[2]

The Tetra Pak recycling proposal for Tetra Brik packaging involves the separation of the paperboard from the polyethylene and aluminum film.[7,8] An overview of this recycling process is shown in Figure 1.

The cellulose separation is performed on an instrument called a hidrapulper, and the recovered paperboard is used to produce industrial paper products such as corrugated cartons and consumer products such as paper towels and notebooks.[8] After the cellulose fiber separation, the remaining mixture, composed of polyethylene, copolymer, and aluminum, is washed in water, pressed, and dried before being subjected to the agglutination process.

The recovery of the polyethylene/aluminum composite can be performed in three different ways: (1) the generation of energy through incineration in a biomass oven, (2) the recovery of aluminum in pyrolysis ovens, and (3) the processing of the mixture of plastic and metal in an extruder to obtain a composite that is used in the fabrication of injection-molded parts as a replacement for LDPE and HDPE.[7]

EXPERIMENTAL

Materials

The material under investigation is PEAL, a composite of LDPE containing a small amount of EMMA and around 15% aluminum, obtained from the recycling of postconsumer aseptic packaging and supplied by Mercoplás (Vinhedo, Brazil). For comparison, pure virgin LDPE and EMMA, supplied by Brasken (Triunfo, Brazil) and used in the composition of multilayer packaging, were also characterized. Descriptions and some properties of the materials used in this work are given in Table I.[9,10]

Processing

The composite PEAL, received in a granulated form, was processed in a Wortex (Campinas, Brazil) single-screw, vented extruder with five temperatures zones. The screw profile was the one typically used for polyolefins and contained a Maddock dispersive mixture element. The screw length/diameter ratio was 30 : 1, and the diameter was 32 mm. Several processing conditions were tested, and the one that resulted in a good appearance and better mechanical properties was chosen. The processing parameters, such as the temperature profile and screw speed, are presented in Table II. Before extrusion, the granules were dried at 90°C for 2 h.

The composites were then injection-molded in an Arburg (Lossburg, Germany) 221K injection machine to obtain the specimens for tensile and impact tests. The injection conditions are also presented in Table II.

Characterization

Thermogravimetric analysis (TGA) was carried out on a TA Instruments (New Castle, DE) model 2050 ther-

TABLE I
Properties of the Virgin Polymers and PEAL

Polymer	LDPE	EMAA	PEAL
Manufacturer	Braskem	BP Chemicals	—
Grade	BC-818	Novex M 21 N 430	—
Density (g/cm^3)	0.918[a]	0.922[a]	0.90[b]
Methacrylic acid (%)	0	1.2[a]	$\ll$1.2
Electrical conductivity (S/cm)[b]	—	—	1.11×10^{-8}
Thermal conductivity at 20°C (W/m °C)[b,c]	—	—	0.24
Heat capacity at 20°C (J/g °C)[c]			2.657

[a] Product datasheet.
[b] Reference 9.
[c] Reference 10.

TABLE II
Parameters for Extrusion and Injection-Molding Processing

Extrusion parameters	PEAL	
Temperature profile (°C)	140, 150, 175, 160, 165	
Screw speed (rpm)	150	
Injection parameters	PEAL	LDPE and EMAA
Temperature profile (°C)	140, 170, 200, 210, 220	180, 190, 200, 200, 200
Injection speed (cm^3/s)	8	8
	7	7
Injection pressure (bar)	800	800
	700	700
Backpressure (bar)	650	650
Cooling time (s)	23	23
Mold temperature (°C)	25 ± 5	25 ± 5

mogravimetric analyzer. The samples, weighing around 30 mg, were tested under an oxidative atmosphere at a heating rate of 10°C/min according to ASTM Standard E 1641.[11]

The melting and crystallization behavior was studied with a TA Instruments model 2910 differential scanning calorimeter. The samples, weighing around 5 mg, were heated, cooled, and reheated at a rate of 10°C/min from 0 to 300°C.

The crystallinity was calculated from the ratio of the experimental melting enthalpy obtained in the second heating to that of 100% crystalline polyethylene, the theoretical value of which was 270.03 J/g.[12] For measuring the PEAL crystallinity, the aluminum weight, considered to be 15 wt %, was subtracted from the initial weight of the sample.

The tensile properties were characterized with an EMIC (São José dos Pinhas, Brazil) DL2000 universal testing machine with a load of 5000 N and a test speed of 50 mm/min. The injection-molded specimens were conditioned for 72 h at 23 ± 2°C and 44% relative humidity before the testing. The specimen dimensions (165-mm length and 41.6-mm^2 cross area), as well as the test conditions, were chosen according to ASTM Standard D 638.[13] At least eight specimens of the same sample were tested, and eventual discrepant results were eliminated by the application of a *Q* test.[14]

Izod impact tests of notched, injection-molded specimens with dimensions of 63.5 mm × 10 mm × 3.2 mm were made with an EMIC pendulum-type testing machine according to ASTM D 256.[15] The load was 2.7 J, and the temperature was 26 ± 3°C. At least eight specimens of the same sample were tested, and the eventual discrepant results were eliminated by the application of a *Q* test.[14]

Dynamic mechanical analysis was performed with a Rheometrics Scientific (Piscataway, NJ) DMTA V. The rectangular specimens (12 mm × 1.5 mm × 0.4 mm) were cut from the injection-molded bars. The measurements were carried out in the tensile mode at a strain of 0.01%, a frequency of 1 Hz, and temperatures ranging from −140 to 280°C at a heating rate of 5°C/min.

Fourier transform infrared (FTIR) analyses of compression-molded thin films were carried out in a Boimen, Hartman & Braun-Michelson (Quebec, Canada) MB series spectrometer from 400 to 4000 cm^{-1} at a resolution of 4 cm^{-1}. A minimum of 50 scans were averaged.

The melt flow index was characterized with a DSM (São Paulo, Brazil) M-I3 plastometer at 190°C and a load of 2.160 kg, according to ASTM 1238 (procedure B).[16]

Scanning electron microscopy (SEM) was used to determine the distribution of aluminum particles in the extruded and injection-molded PEAL. For this analysis, the surface of a cut at room temperature was analyzed. For the extruded samples, the cut was made perpendicularly to the extrusion flow, and in the injection-molded samples, the cut surface parallel to the injection flow was analyzed. The surfaces were observed with a JEOL (Middleton, WI) T 300 microscope. The image was generated by the backscattering electron sign, and the voltage acceleration was 15 kV.

RESULTS AND DISCUSSION

The composite PEAL, remaining from the recycling of aseptic packaging after the extraction of cellulose fibers, comprises a mixture of three materials: two polymers, LDPE and EMAA, and aluminum. The properties of the composite are here evaluated and compared with those of the two virgin polymers.

The transmittance infrared spectra of thin films of the three polyolefins are presented in Figure 2.

The band at 3000 cm^{-1} is related to the symmetric and asymmetric stretching of CH_2 groups occurring at 2919 and 2851 cm^{-1}, respectively. Besides these typical polyethylene bands, the EMAA copolymer presents at 1720 cm^{-1} a band attributed to the C═O stretching and others at 1236 and 941 cm^{-1} related to the stretching of C—O and C—C of the carboxyl

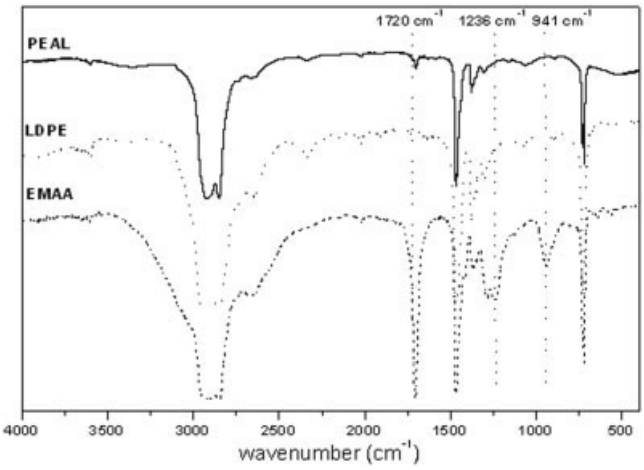

Figure 2 Infrared spectra of PEAL, LDPE, and EMAA (4-cm^{-1} resolution and 50 scans).

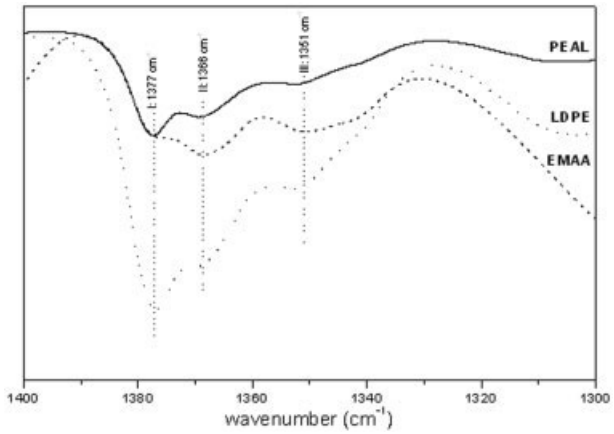

Figure 3 Infrared spectra of PEAL, LDPE, and EMAA from 1300 to 1400 cm^{-1} (4-cm^{-1} resolution and 50 scans).

group. The band at 3000 cm^{-1} becomes broader because of the overlapping of the absorption of the hydroxyl group.

Except for the carbonyl band (1720 cm^{-1}), all the other bands related to the acid group are absent in the PEAL spectrum; this indicates that the amount of the copolymer in the composite is too low to be detected by infrared under the conditions used in this characterization. The presence of the carbonyl band in the PEAL and LDPE spectra is probably a result of polymer oxidation due to the environment and during processing.

Infrared analysis provides the determination of the branching degree and the size of the branches of polyethylene.[17] Band I, at 1377 cm^{-1}, refers to the symmetric deformation of the CH_3 group and is absent for HDPE, which presents this group only in the chain ends. LDPE presents a very high branching degree and a random combination of short and long branches. For this polymer, band I is more intense than band II at 1366 cm^{-1}. This band, as well as the one at 1351 cm^{-1} (band III), is attributed to the deformation of the methylene groups in the amorphous phase.[18] LLDPE presents short branches with a uniform size, the concentration and size of which are determined by the α-olefin amount and type, respectively. In general, the concentration of short branches is lower in LLDPE than in LDPE. For this reason, band II is more intense then band I in the LLDPE infrared spectrum in comparison with the spectrum of LDPE.[17]

A magnification of the region from 1400 to 1300 cm^{-1} of the spectra of Figure 2 is shown in Figure 3. In this region, there is no interference of other absorption. Band II is more intense than band I for EMMA, and this shows that the hydrocarbon chain of EMAA presents few branches and suggests that they are short and uniformly sized branches. Therefore, the hydrocarbon chain of EMAA, one of the polymer constituents of the PEAL composite, presents the characteristics of LLDPE.

Figure 4 presents the thermogravimetric curves of PEAL, LDPE, and EMAA in an oxidant atmosphere. The thermooxidative degradation mechanism is clearly different from that of the two other polymers.

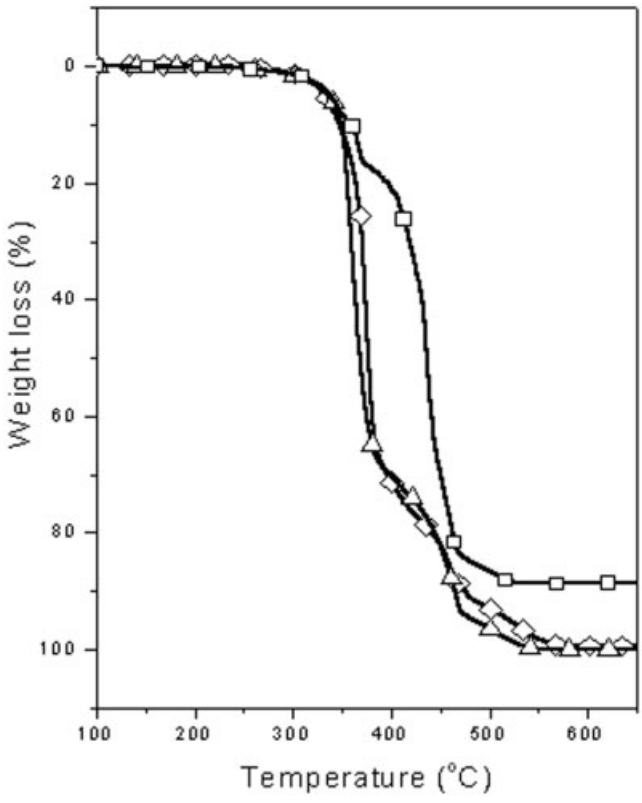

Figure 4 TGA curves for (□) PEAL, (◇) LDPE, and (△) EMAA in an oxidative atmosphere (heating rate = 10°C/min).

TABLE III
Parameters Obtained from the Thermogravimetric and Derivative Curves of LDPE, EMAA, and PEAL Under an Oxidative Atmosphere

	LDPE	EMAA	PEAL
Maximum decomposition temperature (°C)			
First process	374	366	360
Second process	458	436	465
Fraction of weight loss (%)			
First process	69	69	17
Second process	31	31	71
Temperature at which 50% weight loss takes place (°C)	377	368	436
Residue at 600°C in an argon atmosphere (%)	0	0	15

Table III presents the temperature and weight-loss percentage related to each degradation process and the residue at 600°C. LDPE and EMAA showed two well-defined weight-loss processes. PEAL also showed two weight-loss processes; however, an inversion of the percentage of the weight loss in each of the processes can be observed. Although the first degradation process of PEAL started at a temperature slightly lower than that of the other polyethylene, only 17% of the weight was lost, whereas for the other polymers, the first process represented a loss of 69% of the initial weight. The presence of aluminum in the composite then confers higher thermooxidative stability to polyethylene, acting probably as a barrier for oxygen diffusion. In this way, the filler may act as an additive against thermal degradation of the polyolefin; this is an interesting improvement, especially for a recycled polymer subjected to environment and several processing steps. Other important information obtained from the thermogravimetric curves is that the weight loss of polyethylene at the highest processing temperature, 275°C, is insignificant.

The residue shown in the curve of the composite at 600°C, when all the weight of the polymeric matrix had already volatilized, could be used to estimate the aluminum content in the sample. For this consideration, the eventual impurities present in the composite were not taken into account. The average residue weight at 600°C, obtained for the triplicates of thermogravimetric curves obtained in an inert atmosphere (to prevent cross reactions and aluminum oxidation), was 15 ± 2%. This value is in agreement with the average aluminum content in this grade of PEAL (15%).

Figure 5 presents the differential scanning calorimetry (DSC) curves from the first heating, second heating, and cooling obtained for the composite, LDPE, and EMAA.

For all three polymers, the shoulder right before the melting peak, which appears in the first heating curve [Fig. 5(a)], is no longer in the second heating curve [Fig. 5(c)]. The cooling-controlled condition during the DSC run allows higher uniformity in the crystal size and lamellar thickness. This rearrangement in the crystalline structure allows a more gradual variation in the melting of different crystals during the second heating.

The main crystallization peak [Fig. 5(b)] is followed by another less intense and asymmetric peak. This crystallization curve profile is typical for highly branched polyethylenes.

Table IV shows the main thermal parameters obtained through DSC analysis. The crystallinity degree for PEAL was calculated through the subtraction of the weight of the aluminum in the composite.

PEAL presents the highest melting and crystallization temperature as well as the highest crystallinity degree. The crystallization in the composites starts at a temperature higher than that of the other unfilled polyethylene because the aluminum particles act as crystallization nuclei (heterogeneous nucleation). For this same reason, the crystallinity degree in PEAL is higher.

In EMAA, the lower crystallization degree and lower melting and crystallization temperatures in comparison with those of LDPE are related to the presence of the acrylic groups, which interfere with good chain packing.

The dynamic mechanical properties of polyethylenes are expressed through curves of the storage modulus (E'), loss factor (tan δ), and loss modulus (E'') as functions of temperature.

Figure 6(a) shows that the E' curves for all the polymers present two accentuated drops. The one starting at −25°C is attributed to the secondary relaxation of the crystalline phase of polyethylene (β relaxation).[19] The other, at 100°C, is due to the melting of the crystals. Immediately after the melting, in the rubbery region, only the curves for EMAA and PEAL present an elastic plateau, whereas LDPE flows after melting without presenting elastic behavior.

In the case of EMAA, this elastic region is due to the presence of dimers established between the acid groups, which have the same function as physical crosslinking points. In PEAL, besides this same effect, because of the content of EMAA in the composite

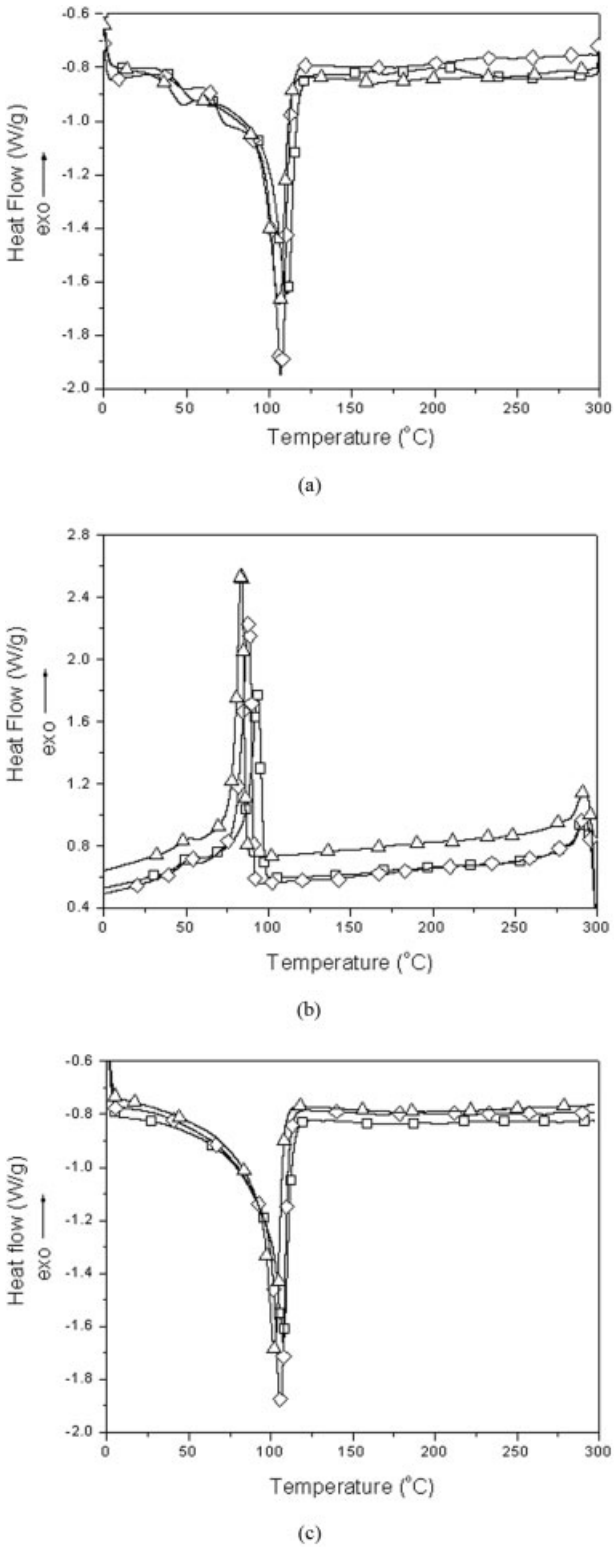

Figure 5 DSC curves for (□) PEAL, (◇) LDPE, and (△) EMAA: (a) first heating, (b) cooling, and (c) second heating (heating rate = 10°C/min).

structure, the presence of aluminum particles provides rigidity to the polymer matrix. This, reducing the flexibility of the polyolefin, also causes a higher modulus at temperatures higher than 0°C. Another factor that contributes to the increase in the modulus is the higher crystallinity of PEAL in comparison with that of LDPE and EMAA (Table IV).

The E'' curves [Fig. 6(b)] present, besides the β relaxation around 0°C, another relaxation around −120°C, which is attributed to the glass transition.[19]

Curves of tan δ as a function of temperature are shown in Figure 6(c). As also observed in Figure 6(a,b), the main difference of the polyethylenes is the width of the β relaxation. For EMAA, this relaxation is presented as a sharp and well-defined peak, whereas PEAL and LDPE show broader and flatter peaks. This result may be related to the differences in the amount and size of branching, as detected through FTIR. The β relaxation is associated with chain segments connecting the crystalline phase to the amorphous phase (tie molecules).[19] Therefore, this relaxation reflects the differences in the branching degree. Those branch segments are normally excluded from the crystalline phase and remain in the interface.

The composite presents a gray color, whereas the pure polymers are slightly white and transparent, the optical transparency of EMMA being higher than that of LDPE. It is also possible to observe the differences in the fracture pattern and in the elongation at break, which follows this sequence: PEAL < LDPE < EMAA. Another detail is the position at which the specimen breaks. In the pure polymers, the tendency is breaking near the clamps, whereas in the composite, the fracture occurs especially in the center of the specimen.

The average stress–strain curves for the composites and pure polymers are presented in Figure 7, and the tensile properties and the Izod impact properties are shown in Table V.

An increase of more than 80% in the PEAL elastic modulus, in comparison with that of the pure polymers, is an indication that the material containing aluminum is stiffer than the other polymers. The higher modulus is related to the presence of aluminum particles and also to the higher crystallinity of the polymer matrix. On the other hand, the material loses toughness because of the metal additive, as indicated by the reduction in the elongation at break. The particles may represent a center for tension concentration.

TABLE IV
Thermal Properties of PEAL, LDPE, and EMAA

Polymer	Melting temperature (°C)	Crystallization temperature (°C)	Crystallinity (%)[a]
PEAL	107	93	47
LDPE	106	88	44
EMAA	102	83	39

The data were obtained from the second heating.
[a] Normalized with respect to the mass fraction of polyethylene in PEAL.

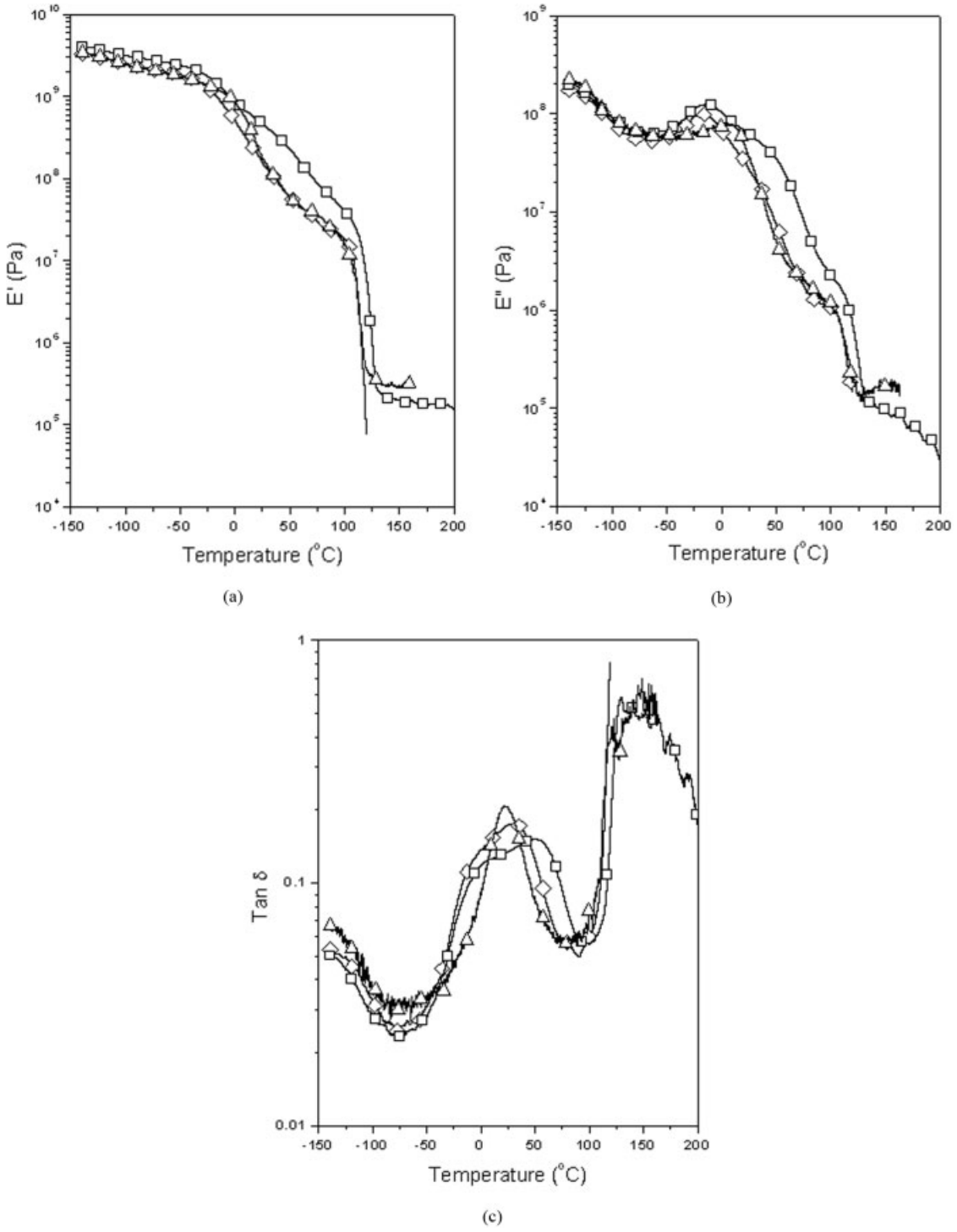

Figure 6 (a) E'), (b) E'', and (c) tan δ as functions of temperature for (□) PEAL, (◇) LDPE, and (△) EMAA.

This reduction in toughness also reflects the impact resistance of the material. The average impact strength for PEAL is 302 J/m. Even though this is a considerably high impact strength, the pure polymers do not fracture under the impact of the pendulum of 1.6 J, which is used in the test. Again, this reduction in the polyethylene impact strength is an effect of the lower flexibility of the composite due to the aluminum particles and also the introduction of interfaces, which may be areas of tension concentration and fracture initial points.

The effects of iron powder,[20–22] cooper,[21,22] zinc,[12,22] and bronze[22] on the physical and mechanical properties of polyethylene have been reported in the literature. In the most cases, the composites present poor mechanical properties and electrical properties de-

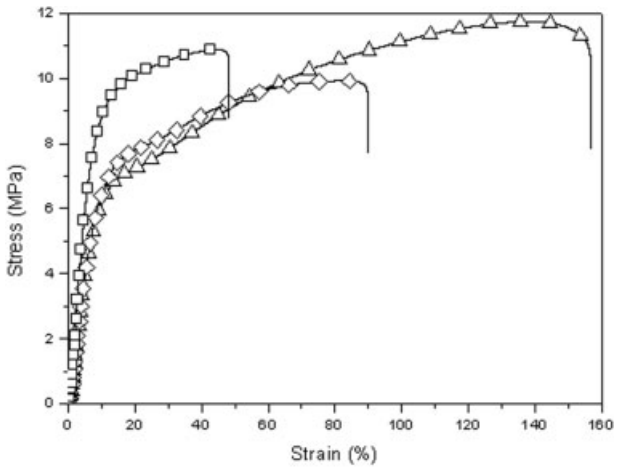

Figure 7 Average stress–strain curves of (□) PEAL, (◇) LDPE, and (△) EMAA.

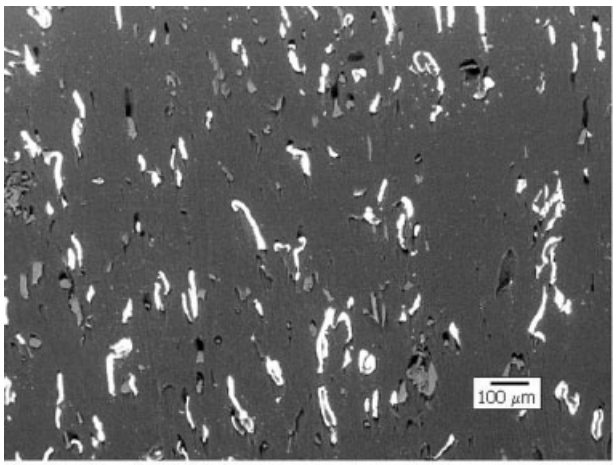

Figure 8 SEM of the surface of injection-molded PEAL: backscattered electron image.

pending on the metal concentration[12,22] and the method of processing.[21]

The melting flow indices found for PEAL, LDPE, and EMAA were 3.9, 7.5, and 7.5 g/10 min, respectively. The values for the virgin polymers were close to the ones presented by the manufacturers, as shown in Table I.

The melting flow index reflects the rheological properties, which are related to the molecular weight and, consequently, the viscosity of the polymeric materials. The melting flow index presented by the composite is lower than that of the virgin polymers. This could be a result of thermal and mechanical degradation caused by the previous use and the recycling process. LDPE may undergo degradation through two different mechanisms: chain scission and crosslinking.[23] Chain scission results in more fluid materials, whereas crosslinking causes an increase in the viscosity and, consequently, a reduction of the melt flow index. However, the composite being a mixture of two polymers and a metallic filler, even the interactions between EMAA and LDPE and between EMAA and aluminum would result in an increase in the viscosity.

The morphology was analyzed through the backscattered electron image, which generated better contrast and definition of the aluminum particle limits.

In Figure 8, it is possible to observe that the particles are long, and the general aspect suggests that many still keep the original film shape, indicating that the processing in the extruder is not effective enough to promote a fine dispersion of the particles. The particle size distribution is quite large, and the average size is approximately 100 μm. However, the filler is homogeneously distributed in the polymer matrix and presents the tendency of orientation along with the injection-flow direction.

CONCLUSIONS

The aluminum particles influence the mechanical and thermal properties as well as the thermal and thermooxidative degradation of polyethylene.

Compared with LDPE, the composite PEAL presents lower fluidity, higher crystallinity, better thermal stability, higher modulus, and lower impact resistance. However, the aluminum particles present a large shape and size distribution that is a negative contribution to the composite properties. Improvements in the processing and dispersion technique are still required for obtaining enhanced performance.

The recycling-originated polymer matrix/metal composite is a very low cost material and shows potential to be used in many applications. In addition, PEAL offers the possibility of being mixed with other thermoplastics for preparing engineering polymer

TABLE V
Mechanical Properties of PEAL, LDPE, and EMAA

	PEAL	LDPE	EMAA
Elongation at break (%)	46 ± 4	92 ± 2	156 ± 3
Stress on maximum strength (MPa)	11 ± 0	10 ± 0	12 ± 0
Young's modulus (MPa)	164 ± 4	93 ± 10	80 ± 12
Impact strength (J/m)	302 ± 4	Not broken	Not broken

blends containing a metallic filler and a compatibilizer.

The authors thank Tetra Pak and Mercoplás for supplying the polymers.

References

1. Castro, F.; Pachione, R. Plast Mod 2002, 334.
2. Hausman, K. In Polymeric Materials Encyclopedia; Salamone, J. C., Ed.; CRC: Boca Raton, FL, 1996; p 1364.
3. Tetra Pak's Official Site. http://tetrapak.com.br (accessed, September 4, 2005).
4. Hara, M.; Sauer, J. A. Rev Macromol Chem Phys 1994, 34, 325.
5. Papadopoulou, C. P.; Kalfoglou, N. K. Polymer 1998, 39, 7015.
6. Mastio, R. C. Modern Plastics Encyclopedia; McGraw Hill: New York, 1999.
7. Neves, F. L. Papel 1999, 64, 36.
8. Zuben, F. V. Coletânea de Trabalhos do III Seminário Internacional de Reciclagem do Alumínio; São Paulo, Brazil, 1996; pp 147–152.
9. Lopes, C. M. A. Ph.D. Thesis, Universidade Estadual de Campinas, 2003.
10. Lopes, C. M. A.; Felisberti, M. I. Polym Testing 2004, 23, 637.
11. Standard Test Method for Decomposition Kinetics by Thermogravimetry; ASTM E 1641-98; American Society for Testing and Materials: West Conshohocken, PA, 1998.
12. Rusu, M.; Sofian, N.; Rusu, D. Polym Testing 2001, 20, 409.
13. (a) Standard Test Methods for Determining the Izod Pendulum Impact Resistance of Plastics; ASTM D 256-98; American Society for Testing and Materials: West Conshohocken, PA, 1998; (b) Standard Test Method for Tensile Properties of Plastics; ASTM D 638-98; American Society for Testing and Materials: West Conshohocken, PA, 1998.
14. Skoog, D. A.; West, D. M.; Holler, F. J. Fundamentals of Analytical Chemistry, 6th ed.; Sanders: Philadelphia, 1992.
15. (a) Standard Test Method for Tensile Properties of Plastics; ASTM D 638-98; American Society for Testing and Materials: West Conshohocken, PA, 1998; (b) Standard Test Method for Melt Flow Rates of Thermoplastics by Extrusion Plastometer; ASTM D 1238-97; American Society for Testing and Materials: West Conshohocken, PA, 1997.
16. Standard Test Method for Melt Flow Rates of Thermoplastics by Extrusion Plastometer; ASTM D 1238-97; American Society for Testing and Materials: West Conshohocken, PA, 1997.
17. Gulmine, J. V.; Janissek, P. R.; Heise, H. M.; Akcelrud, L. Polym Testing 2002, 21, 557.
18. Koenig, J. L. Spectroscopy of Polymers; Elsevier: London, 2000.
19. McCrum, N. G.; Read, B. E.; Williams, G. Anelastic and Dielectric Effects in Polymeric Solids; Dover: Mineola, NY, 1991.
20. Rusu, M.; Sofian, N.; Rusu, D.; Neagu, E.; Neagu, R. J Polym Eng 2001, 21, 469.
21. Mamunya, Y. P.; Muzychenko, Y. V.; Pissis, P.; Lebedev, E. V.; Shut, M. I. J Macromol Sci Phys 2001, 40, 591,
22. Sofian, N. M.; Rusus, M.; Neagu, R.; Neagu, E. Compos Mater 2001, 14, 20.
23. Albertsson, A. C.; Karlsson, S. ACS Symp Ser 1990, 433, 60.